ISIJ International, Vol. 52 (2012), No. 10, pp. 1832–1840

Effects of Ti Addition on Austenite Grain Growth during Reheating of As-Cast 0.2 mass% Carbon Steel

Munekazu OHNO,[1)]* Chihiro MURAKAMI,[2)] Kiyotaka MATSUURA[1)] and Kohichi ISOBE[3)]

1) Division of Materials Science and Engineering, Faculty of Engineering, Hokkaido University, Kita 13 Nishi 8, Kita-ku, Sapporo, Hokkaido, 060-8628 Japan. 2) Graduate Student, Graduate School of Engineering, Hokkaido University, Kita 13 Nishi 8, Kita-ku, Sapporo, Hokkaido, 060-8628 Japan. 3) Muroran R&D Lab., Nippon Steel Corp., 12 Nakamachi Muroran, 050-8850 Japan.

(*Received on March 5, 2012; accepted on May 9, 2012*)

Effects of Ti addition on grain growth in reversely-transformed austenite structure during reheating of the as-cast 0.2 mass% C steel have been investigated for a Ti concentration range between 0 and 0.2 mass% and heating rates from 0.014 to 2.5°C/s. The austenite grain growth during reheating is retarded by the Ti addition and such an effect becomes stronger with the addition of higher amount of Ti. This retarding effect is ascribable to the pinning effect of fine Ti(C,N) particles which should precipitate from the as-cast structure during the reheating process. The experimental results on the grain growth behavior are well explained by the grain growth model including the Zener force and counting reduction of the pinning effect due to the existence of the coarse Ti(C,N) particles crystallized during the solidification.

KEY WORDS: austenite grain structure; pinning effect; reverse transformation; casting; grain growth.

1. Introduction

The refinement of as-cast austenite (γ) grain structure in continuous casting of carbon steels is an important subject to prevent the occurrence of surface cracking of the slabs.[1–2)] During continuous casting, a part of the slab especially in the vicinity of the surface is cooled below A_1 temperature and then reheated due to heat flow from the central part of the slab where the liquid phase still exists. This reheating causes reaustenization from a low temperature structure, viz., α-ferrite + pearlite, bainite or martensite structure. In addition, the reaustenization occurs during heating for the subsequent hot rolling, carburizing, nitriding and the other heat treatments. The behavior of γ grain growth during reheating is an essential factor in the design of several processes following the continuous casting. Hence, the control of the reversely-transformed γ grain structure as well as the as-cast γ grain structure is of critical importance in production of carbon steels.

During the casting process of peritectic carbon steels, the grain growth of γ phase takes place immediately after the completion of transformation into γ single phase at a temperature which is denoted as T_γ.[3–5)] One of possible methods for refining the as-cast γ grain structure is to utilize a pinning effect to prevent the γ grain growth. Our recent study demonstrated that the addition of Ti is effective in reducing the size of as-cast γ grains in 0.2 mass% C steel which is prone to exhibit coarse γ grains because of its high value of T_γ.[6)] **Figure 1** shows the phase diagram of Fe-0.2 mass% C-0.006 mass%

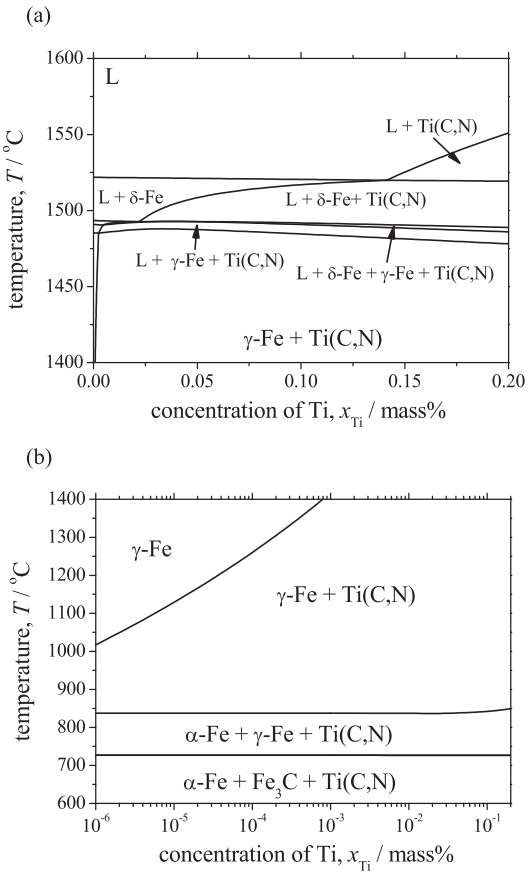

Fig. 1. Calculated phase diagrams of Fe-0.2 mass% C-0.006 mass% N-x_{Ti}Ti in (a) high temperature and (b) low temperature regions. The concentration of Ti in (b) is shown on a logarithmic scale.

* Corresponding author: E-mail: mohno@eng.hokudai.ac.jp
DOI: http://dx.doi.org/10.2355/isijinternational.52.1832

N-x_{Ti}Ti calculated by the CALPHAD method[7] with a thermodynamic database reported in Ref. 8). It was found that during the solidification of the Ti-added steels, N-rich Ti(C,N) particles of facet shape crystallizes in liquid + δ + Ti(C,N) phase field and C-rich Ti(C,N) particles of filmy shape appears from the last-solidifying liquid in liquid + γ + Ti(C,N) phase field. Importantly, the grain refinement by Ti addition is entirely ascribed to the pinning effect of the filmy-shaped Ti(C,N). For instance, the as-cast γ grain size is reduced from about 4 to 2 mm by the addition of 0.1 mass% Ti.

As mentioned above, the reaustenization is generally involved in production of steels and it is important to refine the reversely-transformed γ grain structure. The phase diagram in Fig. 1(b) shows that the addition of Ti stabilizes Ti(C,N) which, for example, exists up to 1 400°C in the steel with 10^{-3} mass% Ti. A number of studies[9–16] have demonstrated that the addition of Ti is effective in inhibiting the γ grain coarsening during isothermal holding and heating processes. This inhibition is attributed to the pinning effect of TiC,[9,13,16] TiN,[9,11–15] Ti(C,N)[10] or the other Ti-based precipitates.[16] Moreover, the coarsening behavior of the precipitates in γ phase, which is an important factor in controlling the pinning effect, has been investigated in detail experimentally[12,15,16] and theoretically.[12,14–16] However, little has been addressed regarding the effect of as-cast structure on the reversely-transformed γ grain structure in Ti-added steels. Although the size of as-cast γ grains (~mm) is generally several orders of magnitude larger than the typical size of reversely-transformed γ grains (10–10^2 μm), the size and morphology of the initial structure for reheating process is affected by those of the as-cast γ grain structure. More importantly, as mentioned above, the crystallized Ti(C,N) phase which prevents the as-cast γ grain growth exists in the as-cast 0.2 mass% C steel with Ti addition. The existence of such a Ti(C,N) phase may alter the precipitation kinetics of fine Ti(C,N) particle which is expected to yield the pinning effect during reheating. Therefore, it is important to investigate the behavior of γ grain growth during reheating of the as-cast Ti-added steel with a particular attention directed at its relevance to the as-cast structure.

In this study, we investigate effects of Ti addition on γ grain growth during reheating of the as-cast 0.2 mass% C steel. It will be shown that the γ grain growth during reheating is retarded by Ti addition and such an effect becomes stronger with the addition of higher amount of Ti. This retarding effect is ascribable to the pinning effect of fine Ti(C,N) particles which should precipitate from the as-cast structure during reheating process. The experimental results on the grain growth behavior are well explained by the grain growth model including the Zener force and taking into account reduction of pinning effect due to the existence of the crystallized Ti(C,N).

2. Experimental

We carried out heating experiments of 0.2 mass% C steel. **Table 1** shows the chemical composition of a 0.2 mass% C steel rod with a diameter of 26 mm employed in this study. A sponge Ti of 99.5% purity was used as the additive material and our focus was placed on a range of Ti addition between 0 and 0.2 mass%. The sample of 300 g was put in an Al_2O_3 crucible with an inner diameter of 35 mm and a depth of 150 mm. The sample was melt at 1 550°C in a SiC furnace filled with Ar gas of five-nine purity and held for 1 h at 1 550°C, followed by cooling at a rate of 0.03°C/s. When the temperature reached 1 100°C, the sample was put out of the furnace and it was cooled to room temperature. This melting and cooling processes are the same as those reported in the previous study for the investigation of effects of Ti addition on the as-cast γ grain structure,[6] except that the sample was air cooled to obtain α + pearlite structure in this study. The average cooling rate during the air cooling was 0.76°C/s. The as-cast sample has a cylindrical shape with a diameter of 35 mm and a height of 90 mm. It was transversely cut into a disk shape with a thickness of 10 mm. Some of the cut pieces were used for the microstructural observation to measure the as-cast γ grain size.

Table 1. Chemical composition of steel (in mass%).

C	Si	Mn	P	S	Al	O	N
0.19	0.20	0.80	0.015	0.007	0.040	0.002	0.006

The disk-shaped sample was vertically cut into four wedge-shaped pieces and the wedge-shaped samples were used for the reheating experiments. The reheating experiments were performed for three different heating rates, 0.014, 0.25 and 2.5°C/s. The reheating experiment for $\dot{T}$ = 0.014°C/s was performed in the SiC furnace. The sample inside an Al_2O_3 crucible was put in the furnace kept at 650°C and then reheated for austenization at a heating rate of $\dot{T}$ = 0.014°C/s. The sample was quenched into strongly stirred iced water from several temperatures ranging between 740 and 1 400°C.

The reheating experiments for $\dot{T}$ = 0.25 and 2.5°C/s were carried out using an infrared gold image furnace. The wedge-shaped sample was put in the Al_2O_3 crucible inside a graphite crucible with an inner diameter of 40 mm and a height of 125 mm. The temperature of the sample was monitored by a K-type thermocouple whose tip was put in the center position of sample. The reheating was conducted from room temperature under an Ar flow condition and the sample was quenched from several temperatures into strongly stirred iced water. Also, in order to investigate the effect of heating rate on the transformation temperatures, the temperature measurement of the sample was carried out for various heating rates.

The quenched sample was sectioned. An aqueous solution of picric acid was used to reveal the γ grain boundary. The microstructural observation was performed by means of an optical microscope and a Scanning Electron Microscope (SEM). Also, a Transmission Electron Microscope (TEM) with an extraction replica technique was used to detect fine particles in the reheated sample as well as the as-cast sample. The chemical composition of the particles was identified by an Electron Probe Micro Analyzer (EPMA) and an Energy Dispersion X-ray Spectroscopy (EDS).

3. Results and Discussion

3.1. Initial Microstructure and Reverse Transformation

Figures 2(a) and 2(b) represent the initial microstructures in the samples without Ti and with 0.1 mass% Ti, respec-

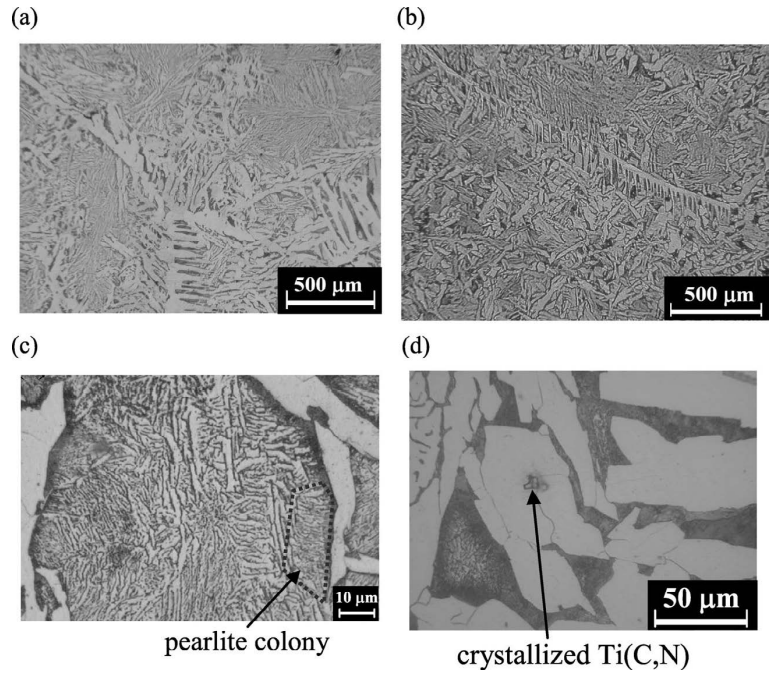

Fig. 2. Initial α + pearlite structures in the samples (a) without Ti and (b) with 0.1 mass% Ti. High magnification images of initial structures in the samples (c) without Ti and (d) with 0.1 mass% Ti.

Table 2. Pearlite colony size and its lamellar spacing in initial structures.

	without Ti	with 0.1 mass% Ti
Pearlite colony size	230 μm	220 μm
Lamellar spacing of pearlite	0.4 μm	0.4 μm

tively. These structures consist of proeutectoid α and pearlite. The high magnification image of the pearlite structure in the sample without Ti is shown in Fig. 2(c). The measured values of pearlite colony size and the lamellar spacing of pearlite in the initial structures are shown in **Table 2**. It was difficult to clearly distinguish between the pearlite structure and acicular-shaped ferrite phases in some regions of the samples and, hence, we selected pearlite structures which were obviously identified in terms of the size and shape and measured their colony sizes and the lamellar spacing. The addition of 0.1 mass% Ti does not lead to substantial changes in pearlite colony size and lamellar spacing of pearlite. As discussed in our previous report,[6] the prior γ grain size is reduced from about 4 mm to about 2 mm by the addition of 0.1 mass% Ti. Furthermore, the size of proeutectoid α phase, which is acicular shape, is slightly reduced by Ti addition in Fig. 2.

It was reported that in the reverse transformation from α + pearlite structure, γ phase preferentially nucleates at the pearlite colony boundary,[17–19] at α/pearlite boundary[20] and also at α/cementite interface inside a pearlite colony.[18] A recent investigation demonstrated that among the pearlite colony boundaries, high angle boundaries between α grains are the preferential nucleation site of γ phase in Fe-0.6 mass%C-0.97 mass%Cr alloy, initial microstructure of which consists of pearlite and about 1% proeutectoid α phase.[21] After the nucleation, γ phase grows into the pearlite until the pearlite dissolution is completed and then, the isolated α phase transforms into γ phase, resulting in the formation of γ grain structure. In the light of these evidences, it is expected that the slight reduction of size of proeutectoid α shown in Fig. 2 might yield a slightly large number of nucleation sites for γ phase in the Ti-added sample. As discussed later, however, this slight difference in the initial microstructure does not produce obvious differences in Ac_1 and Ac_3 temperatures and γ grain size in the early stage of reverse transformation.

As mentioned in the introduction, Ti(C,N) particles appear during the solidification of the Ti-added steel sample. The facet-shaped Ti(C,N) particles crystallize in liquid + δ + Ti(C,N) three-phase field, whereas the filmy-shaped Ti(C,N) particles forms in liquid + γ + Ti(C,N) three-phase field. The latter Ti(C,N) particle prevents γ grain growth during cooling, which results in the refinement of the as-cast γ grain structure. Both types of the Ti(C,N) particles are more than several μm in size and the distances between the particles are a few mm. Figure 2(d) is high magnification image of initial structure in the sample with 0.1 mass% Ti. As indicated by the arrow, coarse Ti(C,N) particle, which corresponds to the facet-shaped Ti(C,N), exists in the initial structure. In the present study, an obvious change in size of these Ti(C,N) particles during cooling was not observed. Importantly, the FE-SEM and extraction replica TEM observations showed that any fine particle of Ti(C,N) (less than 1 μm) does not exist in the Ti-added sample cooled to room temperature, viz., the precipitation of fine Ti(C,N) particles did not take place during the cooling process after solidification.

Ac_1 and Ac_3 temperatures obtained from the heating curves of samples without Ti and with 0.1 mass% Ti are shown in **Fig. 3**. The horizontal dotted and dashed lines represent the equilibrium A_3 and A_1 temperatures, respectively, obtained from the thermodynamic calculations. Both Ac_3 and Ac_1 temperatures slightly increase with the increase in heating rate. There are virtually no differences in Ac_3 and

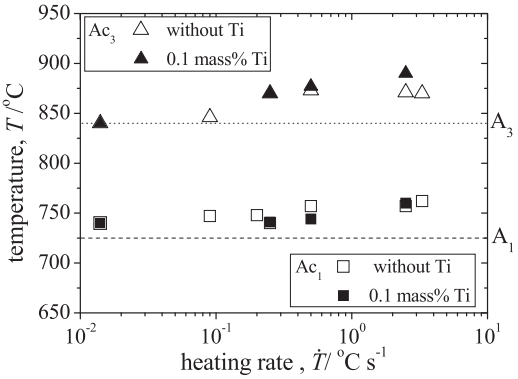

Fig. 3. Heating rate dependences of Ac_1 and Ac_3 temperatures in samples without and with Ti. The horizontal dotted and dashed lines indicate A_3 and A_1 temperatures for the sample without Ti, respectively, obtained by the thermodynamic calculation.

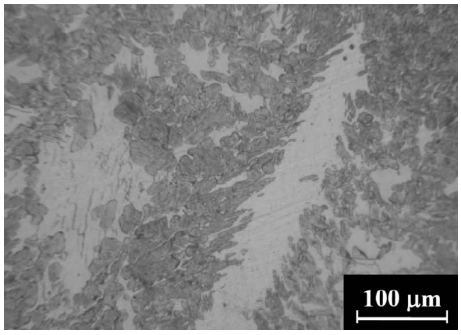

Fig. 4. Microstructure in the sample without Ti, quenched from 800°C during heating at $\dot{T}$ = 0.014°C/s.

Ac_1 temperatures between the samples without and with Ti. Hence, the temperatures for the onset and completion of the reverse transformation are not significantly affected by Ti addition.

Figure 4 shows the microstructure in the sample without Ti quenched from 800°C during heating at $\dot{T}$ = 0.014°C. The bright region corresponds to α phase and the dark region is γ phase. At this temperature, the pearlite structure does not exist. Although not shown here, the area fraction of γ phase was estimated from the microstructural analysis and no difference between the samples without and with Ti was observed regarding the dependence of area fraction of γ phase on the temperature. However, the difference appears in γ grain size in the late stage of reverse transformation. In Fig. 4, the dark region corresponding to γ phase consists of several small γ grains. We measured the γ grain size during the reverse transformation at $\dot{T}$ = 0.014°C/s and the results are plotted in **Fig. 5**. It is seen that the γ grain size gradually increases with increasing temperature from Ac_1. At the beginning of reverse transformation, there is no difference in the γ grain size between the samples with and without Ti. However, the difference in γ grain size arises during the reverse transformation. The grain size in Ti-added sample is always smaller than that in the sample without Ti. Both the samples consist of only γ phase at 900°C at which the γ grain size in Ti-added sample is about three times smaller than that in the sample without Ti. Hence, γ grain growth during the reverse transformation is retarded by Ti addition and the initial γ grain structure just after the completion of

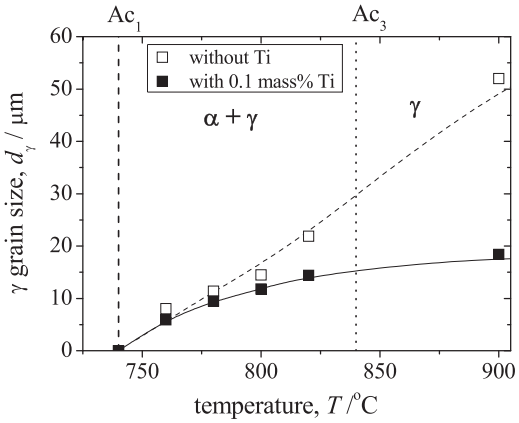

Fig. 5. Temperature dependence of γ grain size in the samples without Ti and with 0.1 mass% Ti during heating process at $\dot{T}$ = 0.014°C/s. The dotted and dashed vertical lines indicate Ac_3 and Ac_1 temperatures, respectively.

the transformation is refined by Ti addition.

As mentioned above, in the as-cast sample with Ti addition before reheating, there are only coarse Ti(C,N) particles formed during the solidification and fine Ti(C,N) particles (less than 1 μm) were not found. Because the coarse Ti(C,N) particles are distributed with the interparticle distance of a few mm, they should not be relevant to the retardation of γ grain growth during the reverse transformation observed in Fig. 5. As demonstrated later, fine Ti(C,N) particles exist in the reheated sample, which is considered to provide the pinning effect on γ grain growth. The results of Fig. 5 imply the fact that the fine Ti(C,N) particles should precipitate before or during the reverse transformation and the pinning effect starts during the reverse transformation.

3.2. Reversely-transformed γ Grain Structure

Figures 6(a) and 6(b) show the reversely-transformed γ grain structures in the samples without Ti and with 0.1 mass% Ti, respectively, heated up to 1 000°C at $\dot{T}$ = 0.014°C/s. It is observed that the addition of Ti significantly reduces the γ grain size. The temperature dependence of γ grain size is shown in **Fig. 7** where the data for low temperature region ($T \leq$ 900°C) correspond to those shown in Fig. 5. The grain size in the sample without Ti gradually increases with the increase in temperature, reaching about 2 mm at 1 400°C. In the Ti-added sample, the grain growth is not significant and the grain size is about four times smaller than that in the sample without Ti at 1 400°C. Hence, the grain growth is retarded up to high temperature region by Ti addition.

The concentration dependences of γ grain size at three different temperatures are shown in **Fig. 8**. The heating rate is $\dot{T}$ = 0.014°C/s. At 1 000°C, the addition of 0.005 mass% Ti significantly reduces the γ grain size from about 70 μm to 20 μm. The further addition of Ti does not yield a substantial change and γ grain size is as low as 20 μm. At the higher temperature of 1 200°C, the grain size increases over the whole concentration range. At this temperature, the grain size is reduced to 30 μm by the addition of more than 0.05 mass% Ti. At 1 400°C, the grain size gradually decreases with increase in Ti concentration. **Figure 9** represents the effect of isothermal holding. By holding at 1 200°C

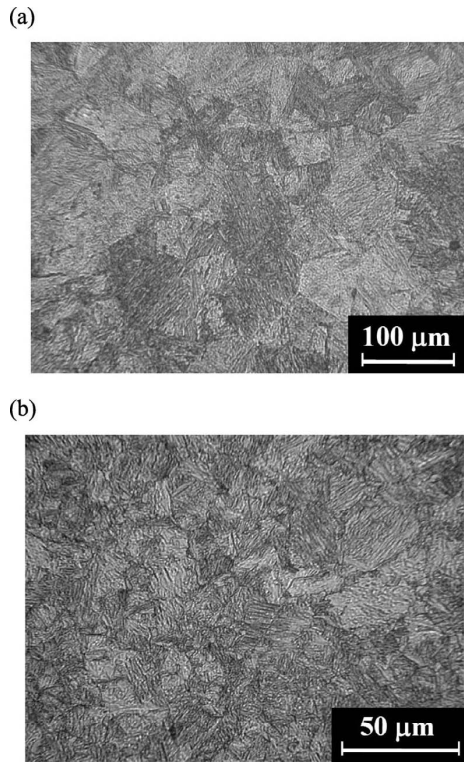

Fig. 6. Reversely-transformed γ grain structures (a) without Ti and (b) with 0.1 mass% Ti heated up to 1 000°C at $\dot{T}$ = 0.014°C/s.

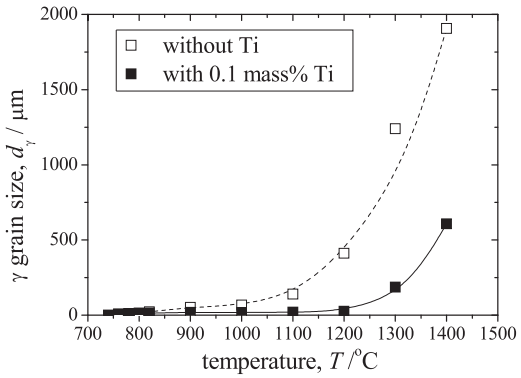

Fig. 7. Temperature dependence of γ grain size in the samples without Ti and with 0.1 mass% Ti during heating process at $\dot{T}$ = 0.014°C/s.

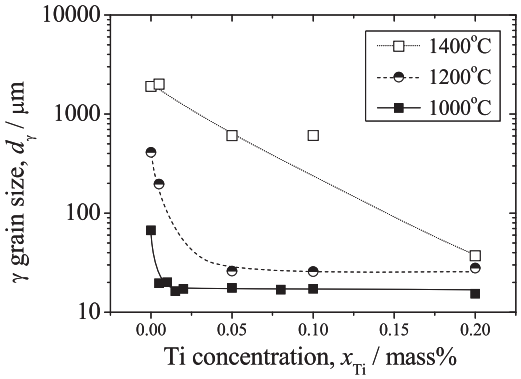

Fig. 8. Concentration dependences of γ grain size at three different temperatures. The heating rate is $\dot{T}$ = 0.014°C/s. The vertical axis is shown on a logarithmic scale.

for 10 hrs, the grain size increases over the whole concentration range. However, the refinement effect by Ti addition still exists even after holding for 10 hrs.

Figure 10 demonstrates the dependence of γ grain size on the heating rate. All the samples were heated up to 1 000°C without holding. In the sample without Ti, the γ grain size was reduced by increasing the heating rate, which should be mainly because the grains growth occurs for a shorter time of period when the heating rate is higher. The grain size is also reduced by increasing the heating rate in the Ti-added sample. Although this reduction is not considerable, the grain size in the Ti-added sample is always smaller than that in the sample without Ti in the range of heating rate we focused on.

It has been known that the γ grain size can be reduced by

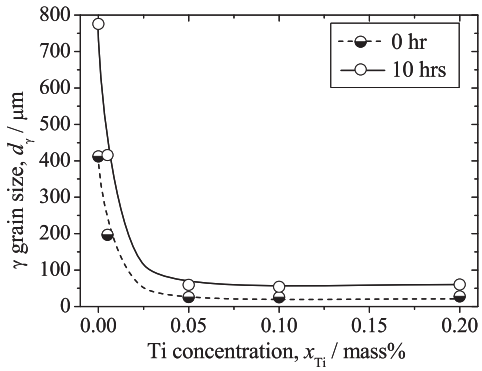

Fig. 9. Concentration dependence of γ grain size in the sample held at 1 200°C for 0 and 10 hours.

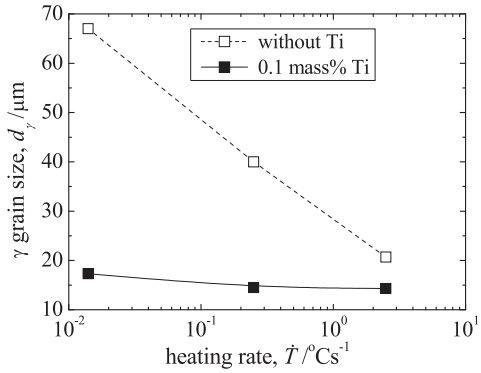

Fig. 10. Dependence of γ grain size on heating rate. The quenching temperature is 1 000°C.

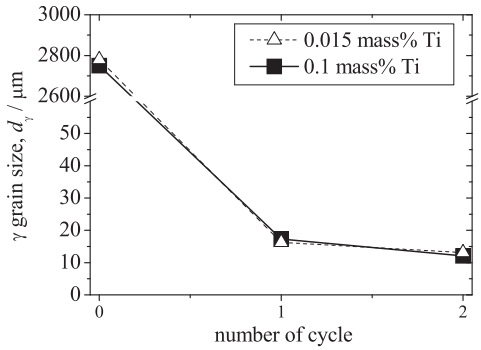

Fig. 11. Effect of the number of heating on γ grain size in the samples with 0.015 and 0.1 mass% Ti. The reheating temperature is 1 000°C and the heating rate is 0.014°C/s.

repeating the reverse transformation due to the refinement of initial microstructure.[22] The dependence of γ grain size on the number of reheating cycle is shown in **Fig. 11**. The grain size at the reheating cycle of zero corresponds to the as-cast grain size. One can see that the γ grain size is significantly reduced by one cycle and it is further reduced by the second cycle. However, the reduction by the second cycle is not substantial and, therefore, we did not carry out the larger number of cycle experiments.

3.3. Pinning Effect of Ti(C,N)

It was demonstrated in the previous subsection that Ti addition significantly reduces the γ grain size during the reheating process. **Figure 12** is the SEM image of the sample with 0.2 mass% Ti heated up to 1 200°C. This is the etched structure. There are many bright particles of a few hundreds nm in size dispersed in this structure. From EPMA and EDS analyses, these particles were identified as Ti(C,N) phase. As mentioned above, Ti(C,N) particles except for the crystallized Ti(C,N) particles were not found in the initial microstructure before the reheating process. Hence, α phase should be supersaturated with respect to Ti before reheating and fine Ti(C,N) particles observed in Fig. 12 should have precipitated from the supersaturated matrix during the reheating process. It is considered that these particles may already exist in $\alpha + \gamma$ temperature region during reheating, because the γ grain size is reduced in Ti-added sample in this temperature range as shown in Fig. 5. The fine Ti(C,N) particles as observed in Fig. 12 are called precipitated Ti(C,N) particle in the following discussion.

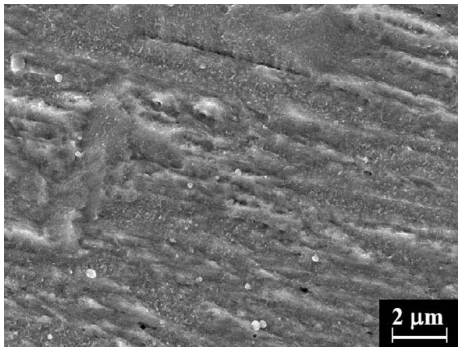

Fig. 12. SEM image of the sample with 0.2 mass% Ti heated up to 1 200°C, showing dispersion of fine Ti(C,N) particles.

The temperature dependence of the equilibrium volume fraction of Ti(C,N), $f^{all}_{Ti(C,N)}$, in the sample with 0.1 mass% Ti is shown in **Fig. 13**. This is the result obtained by the thermodynamic calculations. The vertical dashed line indicates the solidus temperature. $f^{all}_{Ti(C,N)}$ increases during the solidification and in particular, it rapidly increases just before the solidification completes. After the solidification finishes, moreover, $f^{all}_{Ti(C,N)}$ gradually increases with decrease in temperature. $f^{c}_{Ti(C,N)}$ indicates the volume fraction of Ti(C,N) crystallized during the solidification. As mentioned already, the crystallized Ti(C,N) particles are more than several μm in size and an obvious change in size of these Ti(C,N) particles was not observed in the as-cast sample cooled to room temperature. According to these observations, the volume fraction of precipitated Ti(C,N) particles, $f^{p}_{Ti(C,N)}$, can be approximated to be $f^{p}_{Ti(C,N)} = f^{all}_{Ti(C,N)} - f^{c}_{Ti(C,N)}$. The concentration dependence of $f^{all}_{Ti(C,N)}$ at three different temperatures is represented in **Fig. 14**. The addition of Ti gradually increases $f^{all}_{Ti(C,N)}$. As indicated by the bold line, $f^{c}_{Ti(C,N)}$ also increases with increase in Ti concentration.

The theoretical analysis on the effect of the second phase particle on grain growth was first given by Zener.[23] According to the theory, the grain growth is completely inhibited when the grain size reaches a critical grain radius, R_c, given by

$$R_c = \beta \frac{r_p}{f_p}, \quad \text{..... (1)}$$

where r_p and f_p are the radius and volume fraction of the pinning particle, respectively. β in Eq. (1) is a constant given by $\beta = 4/3$. A number of modifications have been proposed for sophistications of the theory and the review was given in Ref. 24). When f_p is less than 0.01, as demonstrated in Ref. 24), R_c of γ grain structure in the presence of second phase particle such as MnS, AlN and (Ti,Nb)CN can be well described by using $\beta = 0.17$.

In order to calculate Eq. (1), we estimated the average radius of Ti(C,N) particle from the microstructural observations. Ti(C,N) particles at high temperatures were relatively large, which enabled an accurate estimation of the particle size. Hence, we first focused on the samples heated up to 1 400°C. We found that the average particle size does not considerably change with the amount of Ti addition and it

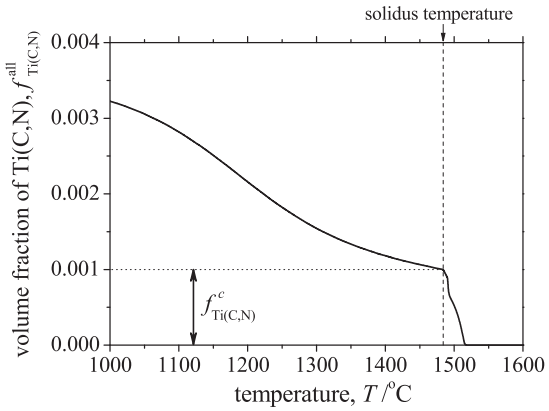

Fig. 13. Temperature dependence of equilibrium volume fraction of Ti(C,N) in the sample with 0.1 mass% Ti. The vertical dashed line indicates the solidus temperature.

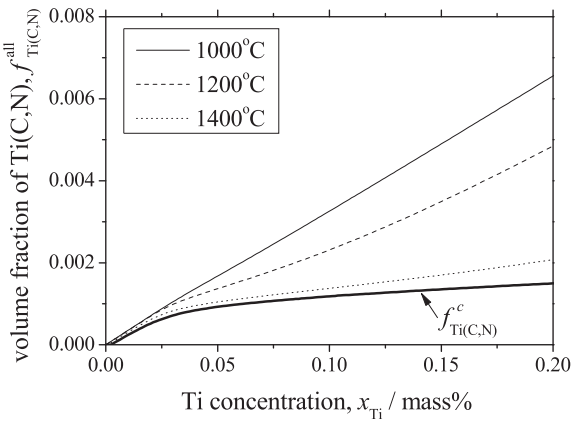

Fig. 14. Concentration dependence of volume fraction of Ti(C,N) in each temperature.

falls within the range of 200–300 nm irrespective of amount of Ti. As for f_p in Eq. (1), we used the values obtained from the thermodynamic calculations. Then, we estimated R_c from Eq. (1) with $\beta = 0.17$. The result is shown in **Fig. 15**. The error bar associated with the estimation of particle radius is added to the calculated result. Two types of the calculated results are shown; one is obtained for $f_p = f^{all}_{Ti(C,N)}$ and the other is obtained for $f_p = f^{p}_{Ti(C,N)}$. One can see that the calculated results for $f_p = f^{p}_{Ti(C,N)}$ reasonably coincide with the experimental data, whereas the calculations for $f_p = f^{all}_{Ti(C,N)}$ underestimate the grain size, namely it overestimate the pinning effect. The comparison in Fig. 15 suggests that the reduction of reheated γ grain size by Ti addition can be explained by the pinning effect of precipitated Ti(C,N) particles.

R_c in Eq. (1), which is called Zener limit, corresponds to a maximum radius that the grains can reach in the presence of second phase particle. In Fig. 15, it was shown that the grain sizes at 1 400°C are well described by the Zener limit in the samples with $x_{Ti} = 0.05$–0.2. During the reheating process, however, the relation given in Eq. (1) generally needs not to be always satisfied and the grain growth in the presence of second phase particle is essentially determined by balance between the driving pressure for grain growth and the pinning pressure induced by the particles. In what follows, we attempt to estimate the temperature range in which the Zener limit is satisfied. We focused on $x_{Ti} = 0.1$ in this analysis.

The grain growth in the presence of the second phase particle can be generally described as,[25]

$$\frac{d}{dt}d_\gamma = m\left(P_{driv} - P_{pin}\right), \quad \text{..... (2)}$$

where m is the mobility of the grain boundary, P_{driv} is the driving pressure for the grain growth as given by

$$P_{driv} = \frac{4\sigma_g}{d_\gamma}. \quad \text{..... (3)}$$

Here, σ_g is the grain boundary energy of γ phase. In Eq. (2), P_{pin} represents the pinning pressure induced by the particle. In this study, P_{pin} is described by the following equation,[25]

$$P_{pin} = 12\sigma_g \frac{f_p}{r_p}, \quad \text{..... (4)}$$

It is important to note that when $dd_\gamma/dt = 0$ is considered, Eqs. (2)–(4) yields the Zener limit identical to Eq. (1) with $\beta = 0.17$. By substituting Eqs. (3) and (4) into Eq. (2), the time evolution equation for d_γ can be rewritten as,

$$\frac{d}{dt}d_\gamma = 4\sigma_g m\left(\frac{1}{d_\gamma} - \frac{3f_p}{r_p}\right) = M\left(\frac{1}{d_\gamma} - \frac{3f_p}{r_p}\right), \quad \text{..... (5)}$$

with $M = 4\sigma_g m$. From Eq. (5), one can determine the temperature region in which Eq. (1) is satisfied. For this, each quantity in Eq. (5) was estimated as explained below.

Our concern is the heating process at a constant heating rate, $\dot{T}$. In Eq. (5), M is dependent on the temperature which is generally expressed as,

$$M(T) = M_0 \exp\left(-\frac{Q^g_{app}}{RT}\right), \quad \text{..... (6)}$$

where M_0 is a constant, Q^g_{app} is the apparent activation energy for the grain growth, R is the gas constant. In order to solve Eq. (5), M_0 and Q^g_{app} need to be determined for the present case. When the second phase particles do not exist, the pinning pressure in Eq. (5) vanishes and then one can obtain the following equation for a constant heating rate,

$$d_\gamma{}^2 - d_{\gamma,0}{}^2 = \frac{2}{\dot{T}}\int_{T_0}^{T} M(T')\,dT', \quad \text{..... (7)}$$

where $d_{\gamma,0}$ is the average grain size at a temperature, T_0. Hence, from Eq. (7), M_0 and Q^g_{app} can be estimated based on the experimental data for γ grain size at several temperatures in the sample without Ti. In the current analysis, M_0 was assumed as $M_0 = 4 \times 10^{-3}$ m^2/s which has been often employed for the analysis on γ grain growth.[26] The value of Q^g_{app} was estimated using the data shown in Fig. 7(open square plots). T_0 was set to 900°C in Eq. (7). Then, Q^g_{app} was estimated as $Q^g_{app} = 230$ kJ/mol. The calculated temperature dependence of d_γ during reheating at $\dot{T} = 0.014$°C/s is compared with the experimental data in **Fig. 16**. The calculated result is in agreement with the experimental data in the temperature region of our focus.

In the Ti-added sample, the pinning pressure by Ti(C,N) particle should exist and f_p and r_p need to be estimated in Eq. (5). Since our focus is a relatively slow heating rate of $\dot{T} = 0.014$°C/s, we assume that the volume fraction of Ti(C,N) reaches the equilibrium value at each temperature and hence

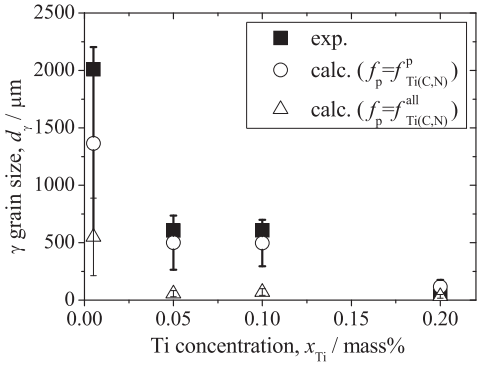

Fig. 15. Comparison between the experimental and calculated results for concentration dependence of γ grain size heated up to 1 400°C.

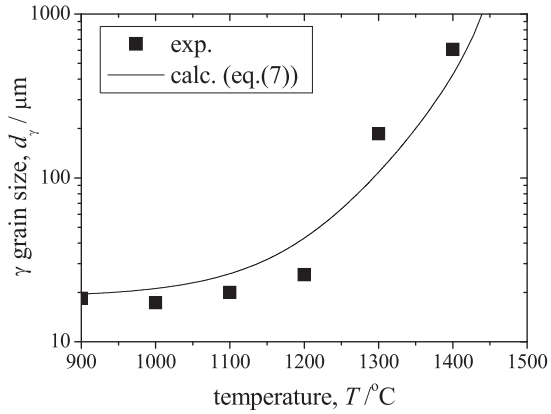

Fig. 16. Comparison between the experimental and calculated results of the temperature dependence of γ grain size during heating at $\dot{T} = 0.014$°C/s in the sample without Ti.

$f_p(T)$ is given as $f_p(T) = f^p_{Ti(C,N)}(T)$ from the thermodynamic calculation. It was reported that the growth of TiN particle in γ grain structure of low-alloyed steels can be well described by the Lifshitz, Slyozov and Wagner's (LSW) theory of Ostwald ripening.[15] When the heating process is considered, the time evolution of r_p can be described based on the LSW theory as follows,

$$r_p^{\,3} - r_{p,0}^{\,3} = \frac{1}{\dot{T}}\int_{T_0}^{T} k(T')\,dT' \quad \text{..... (8)}$$

where $r_{p,0}$ represents the average radius of particle at a temperature T_0. The coefficient $k(T)$ was derived for the growth of carbides in early studies.[27] In the case of carbonitride, $(Fe, X)_a(C,N)_b$ with an element X and site fractions a and b, $k(T)$ can be expressed as,

$$k(T) = \frac{8(a+b)\sigma_I V^p D_X^\gamma u_X^\gamma}{9aRT\left(u_X^p - u_X^\gamma\right)^2}, \quad \text{..... (9)}$$

where σ_I is the interfacial energy between the carbonitride and matrix, V^p is the molar volume of carbonitride (m^3/mole of atom). u_X^i with $i = p$ and γ represents a concentration parameter of the element X in carbonitride and γ phases, respectively, as defined by,

$$u_X^i = \frac{x_X^i}{1 - x_C^i - x_N^i} \quad \text{..... (10)}$$

where x_j^i is the mole fraction of element j in i phase. D_X^γ in Eq. (9) is the diffusion coefficient of element X in γ phase as given by,

$$D_X^\gamma = D_0 \exp\left(-\frac{Q_{app}^p}{RT}\right), \quad \text{..... (11)}$$

where D_0 is a constant and Q_{app}^p is the apparent activation energy for diffusion. In the present case, X = Ti and a = b = 1 in Eq. (9). The constants D_0 and Q_{app}^p were given as $D_0 = 0.15 \times 10^{-4}$ m^2/s[14] and $Q_{app}^p = 21$ kJ/mol.[12] x_j^i was obtained at each temperature from the thermodynamic calculations. V^p was given as $V^p = V^{Ti(C,N)}/2 = 5.9 \times 10^{-6}$ m^3/mol. σ_I was assumed as $\sigma_I = 0.8$ J/m^2 based on the calculated result of nearest-neighbor broken-bond method.[28]

From Eqs. (5) and (8), we calculated the γ grain size at each temperature during reheating process, focusing on $x_{Ti} = 0.1$ and $\dot{T} = 0.014$°C/s. We used the experimental value of $d_{\gamma,0} = 18$ μm at 900°C in Eq. (5) and $r_{p,0} = 180$ nm at 900°C in Eq. (9) which was chosen so that the experimental value of $r_p = 250$ nm at 1 400°C is reproduced from Eq. (9). The calculation was done from low to high temperature until the right-hand side of Eq. (5) becomes null, viz., the driving pressure for grain growth exactly balances the pinning pressure by precipitated Ti(C,N) particle. When the right-hand side of Eq. (5) becomes null, d_γ was calculated based on Zener limit, Eq. (1). The calculated result of d_γ is shown in **Fig. 17** where the experimental data for $x_{Ti} = 0.1$ are also plotted. The dashed and solid lines indicate the results of Eqs. (5) and (1), respectively. The inset is the enlargement of low temperature region. Although a slight difference is observed in high temperature region, the calculated result fairly agrees with the experimental result. Importantly, the Zener limit is not always satisfied. It is satisfied when the temperature is higher than $T = 1\,050$°C in Fig. 17. Below this temperature, the grain growth occurs, overcoming the pinning pressure even though the amount of Ti addition is as high as 0.1 mass%.

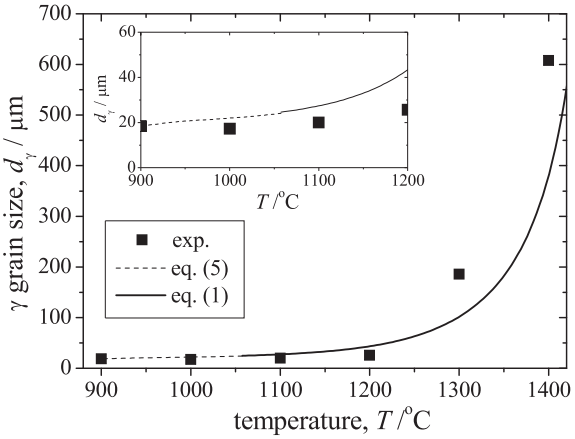

Fig. 17. Comparison between the experiment and the calculated results for γ grain size at several temperatures.

As reported in Ref. 12), the heating rate affects the coarsening kinetics of TiN. The agreement between the calculated and experimental results in Fig. 17 supports that the coarsening kinetics of Ti(C,N) particles in our experiments can be explained by the LSW theory, Eq. (8). Therefore, it is expected that the size of Ti(C,N) particles at a given temperature should decrease with increase in the heating rate according to Eq. (8), which, however, remains to be experimentally investigated in detail in a future study.

The addition of Ti reduces the as-cast γ grain size in 0.2 mass% C steel due to the pinning effect of Ti(C,N) crystallized from the liquid phase. Neither the substantial coarsening of crystallized Ti(C,N) nor precipitation of new Ti(C,N) particle occur during the cooling process in our experiments. In this study, it was found that the fine Ti(C,N) particles appear during reheating of the as-cast sample and the refinement effect of γ grain structure can be explained by the pinning effect of the fine Ti(C,N) particle. Hence the precipitation kinetics of fine Ti(C,N) is important to know for precise control of the pinning effect during reheating process. However, when and where the fine Ti(C,N) particle precipitates during reheating were not clarified and also the reason why the fine Ti(C,N) particle did not form during cooling was not discussed in this study. These remain to be addressed in a future work. Moreover, our analyses showed that the existence of crystallized Ti(C,N) causes less pinning effect, since the volume fraction of precipitated Ti(C,N) is lowered from the equilibrium value by the amount of crystallized one. In other words, although there is a certain amount of the crystallized Ti(C,N) particles in the as-cast γ grain structure, they are too coarse to work as a pin for γ grain growth during reheating and the pinning effect during reheating is provided by the precipitated Ti(C,N) particle, the amount of which is restricted due to the presence of crystallized Ti(C,N) particles. Hence, further refinement of reheated γ grain structure by Ti addition should require the control of the solidification process to make crystallized Ti(C,N) finely dispersed so that the pinning effect of the crystallized Ti(C,N) is utilized during the reheating process.

4. Conclusions

In our recent study,[6] it was demonstrated that the addition of Ti is effective in reducing the size of as-cast γ grains in 0.2 mass% C steel which is prone to exhibit coarse γ grains. The refinement of as-cast γ grain structure by Ti addition is entirely ascribed to the pinning effect of the filmy-shaped Ti(C,N) particle crystallized from the last-solidifying liquid. In this study, we have investigated the effects of Ti addition on γ grain structure during reheating of the as-cast 0.2 mass% C steel, focusing on the range of Ti addition from 0 to 0.2 mass% and three different heating rates, 0.014, 0.25 and 2.5°C/s. The following are important findings,

(1) The initial microstructure of the as-cast steel sample with a cooling rate of 0.03°C/s consists of α + pearlite structure and coarse Ti(C,N) particles crystallized from the liquid phase. There was no fine Ti(C,N) particle (less than 1 μm).

(2) The austenite grain growth during reheating is retarded by Ti addition and the retardation effect starts before the completion of the reverse transformation.

(3) The retardation effect becomes stronger with the addition of higher amount of Ti.

(4) This retarding effect should be ascribable to the pinning effect of fine Ti(C,N) particles which precipitate during reheating process. The experimental results on the grain growth behavior are well explained by the grain growth model including the Zener force and counting reduction of the pinning effect due to the existence of the crystallized Ti(C,N).

Acknowledgement

This work is supported by Grant-in-Aid for Young Scientists (A) (No. 22686067) from MEXT, Japan.

REFERENCES

1) B. Mintz and J. M. Arrowsmith: *Met. Technol.*, **6** (1979), 24.
2) L. Schmidt and Å. Josefsson: *Scand. J. Metall.*, **3** (1974), 193.
3) Y. Maehara, K. Yasumoto, Y. Sugitani and K. Gunji: *Trans. Iron Steel Inst. Jpn.*, **25** (1985), 1045.
4) K. Yasumoto, T. Nagamichi, Y. Maehara and K. Gunji: *Tetsu-to-Hagané*, **73** (1987), 1738.
5) N. S. Pottore, C. I. Garcia and A. J. DeArdo: *Metall. Trans. A*, **22A** (1991), 1871.
6) S. Tsuchiya, M. Ohno, K. Matsuura and K. Isobe: *Tetsu-to-Hagané*, **95** (2009), 629.
7) L. Kaufman and H. Bernstein: Computer Calculation of Phase Diagrams with Special Reference to Refractory Materials, Academic Press, New York, (1970), 1.
8) B. J. Lee: *Metall. Mater. Trans. A*, **32A** (2001), 2423.
9) A. Adachi, K. Mizukawa and K. Kanda: *Tetsu-to-Hagané*, **49** (1963), 894.
10) T. Watanabe, S. Fukui, K. Katô and C. Asada: *Electric Furnace Steel*, **39** (1968), 96.
11) S. Kanazawa, A. Nakashima, K. Okamoto and K. Kanaya: *Tetsu-to-Hagané*, **61** (1975), 2589.
12) S. Matsuda and N. Okumura: *Tetsu-to-Hagané*, **62** (1976), 1210.
13) H. Kobayashi and Y. Kasamatu: *Tetsu-to-Hagané*, **67** (1981), 124.
14) P. A. Manohar, D. P. Dunne, T. Chandra and C. R. Killmore: *ISIJ Int.*, **36** (1996), 194.
15) S. F. Medina, M. Chapa, P. Valles, A. Quispe and M. I. Vega: *ISIJ Int.*, **39** (1996), 930.
16) H. Murakami: *Tetsu-to-Hagané*, **89** (2003), 544.
17) S. Kinoshita and T. Ueda: *Tetsu-to-Hagané*, **59** (1973), 1261.
18) D. V. Shtansky, K. Nakai and Y. Ohmori: *Acta Mater.*, **47** (1999), 2619.
19) E. Schmidt, Y. Wang and S. Sridhar: *Metall. Mater. Trans. A*, **37A** (2006), 1799.
20) A. Roósz, Z. Gácsi and E. G. Fuchs: *Acta Metall.*, **31** (1983), 509.
21) Z.-D. Li, G. Miyamoto, Z.-G. Yang and T. Furuhara: *Scr. Mater.*, **60** (2009), 485.
22) T. Furuhara, K. Kikumoto, H. Saito, T. Sekine, T. Ogawa, S. Morito and T. Maki: *ISIJ Int.*, **48** (2008), 1038.
23) C. S. Smith: *Trans. AIME*, **175** (1948), 15.
24) P. A. Manohar, M. Ferry and T. Chandra: *ISIJ Int.*, **38** (1998), 913.
25) K. Banerjee, M. Militzer, M. Perez and X. Wang: *Metall. Mater. Trans. A*, **41A** (2010), 3161.
26) C. Bernhard, J. Reiter and H. Presslinger: *Metall. Mater. Trans. B*, **39B** (2008), 885.
27) M. Y. Wey, T. Sakuma and T. Nishizawa: *Trans. JIM*, **20** (1981), 733.
28) Z.-G. Yang and M. Enomoto: *Metall. Mater. Trans. A*, **32A** (2001), 267.